Generalized Master Equation with Non-Markovian Multichromophoric Förster Resonance Energy Transfer for Modular Exciton Densities

Seogjoo Jang,[1,*] Stephan Hoyer,[2] Graham Fleming,[3,4] and K. Birgitta Whaley[3]
[1]Department of Chemistry and Biochemistry, Queens College and the Graduate Center, City University of New York, 65-30 Kissena Boulevard, Flushing, New York 11367, USA
[2]Department of Physics, University of California, Berkeley, California 94720, USA
[3]Department of Chemistry, University of California, Berkeley, California 94720, USA
[4]Physical Biosciences Division, Lawrence Berkeley National Laboratory, Berkeley, California 94720, USA
(Received 4 July 2013; revised manuscript received 16 September 2014; published 31 October 2014)

A generalized master equation (GME) governing quantum evolution of modular exciton density (MED) is derived for large scale light harvesting systems composed of weakly interacting modules of multiple chromophores. The GME-MED offers a practical framework to incorporate real time coherent quantum dynamics calculations of small length scales into dynamics over large length scales, and also provides a non-Markovian generalization and rigorous derivation of the Pauli master equation employing multichromophoric Förster resonance energy transfer rates. A test of the GME-MED for four sites of the Fenna-Matthews-Olson complex demonstrates how coherent dynamics of excitonic populations over coupled chromophores can be accurately described by transitions between subgroups (modules) of delocalized excitons. Application of the GME-MED to the exciton dynamics between a pair of light harvesting complexes in purple bacteria demonstrates its promise as a computationally efficient tool to investigate large scale exciton dynamics in complex environments.

DOI: 10.1103/PhysRevLett.113.188102 PACS numbers: 87.15.hj, 05.60.Gg, 71.35.−y

Most photosynthetic units of bacteria and higher plants have modular structures where the entire systems are composed of smaller subunits, or "modules" of protein-chromophore complexes [1,2]. While the nature of interactions and quantum dynamics within each module varies, the intermodule interactions in such systems are generally weak. A striking characteristic is that excitons can migrate through those weak links and find their destinations with near unit efficiency within picoseconds. How can this be accomplished despite significant disorder and fluctuations? What are the general conditions ensuring such high efficiency of natural systems? Recent theoretical studies provide some clues [3–7], but the answers for the above fundamental questions are far from being settled. To this end, simulation of exciton dynamics over larger length and longer time scales including realistic effects of disorder or fluctuations is needed. However, accurate quantum dynamical calculations typically apply to small (∼7 chromophores) [8,9] or medium range systems having up to ∼30 chromophores [10–13], with the latter already requiring massive computational resources. Thus, application of such an approach to simulation of complexes with hundreds of chromophores (e.g., photosystem II) also while averaging over a sufficiently large ensemble of disorder is impractical at present. Instead, the Pauli master equation (PME) is frequently used for such calculations [14–20], but without clear derivation of its kernels from quantum dynamical principles. As such, it is difficult to establish a connection between the observed phenomenology and the key microscopic features.

In this work, we derive a generalized master equation (GME) for the time evolution of the exciton density coarse grained over a module, i.e., the modular exciton density (MED). The resulting GME-MED complements a recent analysis of coherence propagation between weakly coupled multichromophore units [6], clarifies assumptions underlying the use of multichromophoric Förster resonance energy transfer (MC-FRET) rate [3,21,22] in a PME, and provides its non-Markovian generalization. We also demonstrate that the GME-MED serves as a practical means to incorporate high level intramodule quantum calculations into energy transfer simulation over significantly longer length scales.

Consider a total Hamiltonian given by $H = H_0 + H_c$, where H_0 represents noninteracting modules of excitons plus their environmental degrees of freedom and H_c the couplings between different modules. Each module is denoted as n or m, and a chromophore in the nth module is denoted as j_n, k_n, etc. Thus,

$$H_0 = \sum_n H_n = \sum_n \left\{ H_n^e + \sum_{i_n, j_n} B_{i_n j_n} |i_n\rangle\langle j_n| + H_n^g \right\}, \quad (1)$$

with H_n^e the single exciton Hamiltonian of the nth module, $|i_n\rangle$ the site excitation state of the i_nth chromophore in the nth module, $B_{i_n j_n}$ the bath operator coupled to the excitonic term $|i_n\rangle\langle j_n|$, and H_n^g the bath Hamiltonian (the

Hamiltonian in the ground electronic state) of the nth module. The intermodule coupling Hamiltonian has the form

$$H_c = \sum_{n,m} \sum_{j_n,k_m} J_{j_n k_m} |j_n\rangle\langle k_m|, \tag{2}$$

where $J_{j_n k_m}$ is assumed to be real and symmetric. By definition, $J_{j_n k_m} = 0$ for $n = m$. For generality, we assume that H_n^e, $B_{i_n j_n}$, and H_c are time dependent (although not shown explicitly) but that H_n^g is time independent. Figure 1 provides a schematic modular structure.

We denote the time evolution operator for the interaction free Hamiltonian H_0 as $U_0(t,t') = \exp_{(+)}\{-i\int_{t'}^{t} d\tau H_0(\tau)/\hbar\} = \prod_n U_n(t,t')$, where $U_n(t,t') = \exp_{(+)}\{-i\int_{t'}^{t} d\tau H_n(\tau)/\hbar\}$ with the subscript $(+)$ implying chronological time ordering. Assuming that the exciton is created at time $t = 0$, we shall abbreviate $U_0(t,0)$ and $U_n(t,0)$ as $U_0(t)$ and $U_n(t)$. The total density operator is denoted as $\rho(t)$. In the interaction picture with respect to H_0, $\rho_I(t) = U_0^\dagger(t)\rho(t)U_0(t)$ evolves according to $\partial\rho_I(t)/\partial t = -i[H_{c,I}(t),\rho_I(t)]/\hbar = -i\mathcal{L}_{c,I}(t)\rho_I(t)$, where $H_{c,I}(t) = U_0^\dagger(t)H_c U_0(t)$. The second equality defines $\mathcal{L}_{c,I}(t)$. The ground state time evolution operator of the nth module is denoted as $U_n^g(t) = \exp\{-itH_n^g/\hbar\}$. Since $|j_n\rangle$ represents the state where only the j_nth chromophore in the nth module is excited while all other modules are in the ground electronic state, $\langle j_n|U_0(t) = (\prod_{m\neq n} U_m^g(t))\langle j_n|U_n(t)$. Thus,

$$H_{c,I}(t) = \sum_{n,m}\sum_{j_n,k_m} J_{j_n k_m}\mathcal{T}_{j_n k_m}(t) = \sum_{n,m}\mathcal{F}_{nm}(t), \tag{3}$$

where $\mathcal{T}_{j_n k_m}(t) = U_n^\dagger(t)U_n^g(t)|j_n\rangle\langle k_m|U_m^{g\dagger}(t)U_m(t)$ and the second equality defines $\mathcal{F}_{nm}(t)$. By definition, $\mathcal{F}_{nm}(t)$ vanishes for $n = m$. We denote the identity operator in the single exciton space of each module as $1_n = \sum_{j_n}|j_n\rangle\langle j_n|$ and that in the total single exciton space as $1 = \sum_n 1_n$. The equilibrium bath canonical density operator of the nth module in the ground electronic state is $\rho_{bn} = e^{-\beta H_n^g}/\mathrm{Tr}_b\{e^{-\beta H_n^g}\}$.

The key idea in deriving the GME-MED is to introduce the following *modular projection* superoperator $\mathcal{P}$:

$$\mathcal{P}(\cdot) = \sum_n \rho_{bC_n}\mathrm{Tr}_{bC_n}\{1_n(\cdot)1_n\}, \tag{4}$$

where $(\cdot)$ represents an arbitrary operator, $\rho_{bC_n} = \prod_{m\neq n}\rho_{bn}$, and Tr_{bC_n} represents the trace over all baths except for those associated with the nth module. The superoperator $\mathcal{P}$ projects the total density operator into an independent sum of blocks, each representing a module, and satisfies the required condition of $\mathcal{P}^2 = \mathcal{P}$. It also satisfies the identity $\mathcal{P}\mathcal{L}_{c,I}(t)\mathcal{P} = 0$ [see Supplemental Material [23]]. We assume a simple initial condition at time $t = 0$ with no intermodule quantum coherence because the likelihood of such a coherent state under natural condition is very small, so that $(1-\mathcal{P})\rho_I(0) = 0$. Then, from the well-known formal solution for $\mathcal{P}\rho_I(t)$ (see [23]), it is easy to derive the following time evolution equation for the total nth module density operator, $\rho_{n,I}(t) = \mathrm{Tr}_{bC_n}\{1_n\rho_I(t)1_n\}$:

$$\frac{\partial}{\partial t}\rho_{n,I}(t) = -\sum_m \int_0^t d\tau 1_n \mathrm{Tr}_{bC_n}\{\mathcal{L}_{c,I}(t) \times e_{(+)}^{-i\int_\tau^t d\tau'(1-\mathcal{P})\mathcal{L}_{c,I}(\tau')}\mathcal{L}_{c,I}(\tau)\rho_{bC_m}\rho_{m,I}(\tau)\}1_n, \tag{5}$$

which is formally exact but not amenable for practical solution yet. Under the assumption that the intermodule coupling H_c is small compared to H_0, the approximation $e_{(+)}^{-i\int_\tau^t d\tau'(1-\mathcal{P})\mathcal{L}_{c,I}(\tau')} \approx 1$ can be made in Eq. (5). This results in the following second-order approximation with respect to H_c:

$$\frac{\partial}{\partial t}\rho_{n,I}(t) = -\sum_m \int_0^t d\tau \times 1_n\mathrm{Tr}_{bC_n}\{\mathcal{L}_{c,I}(t)\mathcal{L}_{c,I}(\tau)\rho_{bC_m}\rho_{m,I}(\tau)\}1_n. \tag{6}$$

The above equation provides a complete prescription to incorporate full quantum dynamics calculations for each module (made using, e.g., the methods of [29,30]) into a consistent description of the dynamics across all coupled modules. Note that the only assumption invoked here is the smallness of H_c compared to H_0. This assumption can be used as long as a natural division into weakly coupled modules exists. This can be justified in most light harvesting supercomplexes, with the possible exception of the chlorosome of the green sulfur bacteria [31], which appears to have an extended network of coupled chromophores. However, even in this case, the excitons have finite coherence lengths due to disorder or exciton-phonon

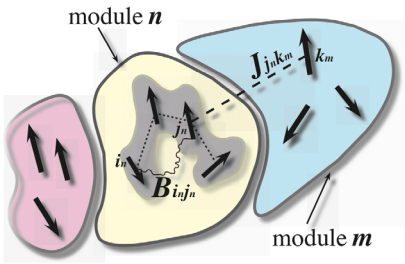

FIG. 1 (color online). Schematic of a modular system. Arrows represent transition dipoles of each chromophore, dotted and dashed lines their electronic couplings (within and between complexes, respectively), and wavy lines exciton-bath couplings. The gray region represents MED.

couplings and application of our formalism may be feasible in this case by appropriately choosing modules comparable to the coherence sizes of excitons [20].

When the main focus is on the exciton states, the equation for the reduced system density operator, $\sigma_{n,I}(t) = \mathrm{Tr}_{bn}\{\rho_{n,I}(t)\}$, can be obtained by tracing Eq. (6) over the bath of the nth module and employing the explicit expression for $H_{c,I}(t)$ of Eq. (3). The result becomes

$$\begin{aligned}\frac{\partial}{\partial t}\sigma_{n,I}(t) = -\frac{1}{\hbar^2}\sum_{m\neq n}\int_0^t d\tau(&\mathrm{Tr}_b\{\mathcal{F}_{nm}(t)\mathcal{F}_{mn}(\tau)\rho_{n,I}(\tau)\rho_{bC_n}\}\\ &+\mathrm{Tr}_b\{\rho_{bC_n}\rho_{n,I}(\tau)\mathcal{F}_{nm}(\tau)\mathcal{F}_{mn}(t)\}\\ &-\mathrm{Tr}_b\{\mathcal{F}_{nm}(t)\rho_{bC_m}\rho_{m,I}(\tau)\mathcal{F}_{mn}(\tau)\}\\ &-\mathrm{Tr}_b\{\mathcal{F}_{nm}(\tau)\rho_{bC_m}\rho_{m,I}(\tau)\mathcal{F}_{mn}(t)\}),\end{aligned} \tag{7}$$

where the fact that $\mathrm{Tr}_{bn}\mathrm{Tr}_{bCn} = \mathrm{Tr}_b$ has been used.

The integrands of Eq. (7) can be related to line shape operators of each module. For this, we introduce the following exciton space operators:

$$\mathcal{I}_n(t,\tau) = \mathrm{Tr}_{bn}\{U_n(t,\tau)1_n\rho_{bn}U_n^{g\dagger}(t-\tau)\}, \tag{8}$$

$$\mathcal{E}_n(t,\tau;\rho_n) = \mathrm{Tr}_{bn}\{U_n^g(t-\tau)\rho_n(\tau)U_n^\dagger(t,\tau)\}, \tag{9}$$

where $\rho_n(\tau) = U_n(\tau)\rho_{n,I}(\tau)U_n^\dagger(\tau)$. The Fourier transform of $\mathcal{I}_n(t,\tau)$ with respect to $t-\tau$ produces the absorption line shape when contracted with transition dipole vectors. A similar procedure with $\mathcal{E}_n(t,\tau;\rho_n)$ leads to the time-dependent emission line shape depending on $\rho_n(\tau)$ as its initial condition. For complete representation of all the integrands of Eq. (7), we need to define additional operators with specific coherence information built in as follows:

$$\begin{aligned}\mathcal{I}_{n,j_n''j_n'''}(t,\tau) = \mathrm{Tr}_{bn}\{&U_n(t-\tau)\\ &\times(U_n(\tau)|j_n'''\rangle\langle j_n''|U_n^\dagger(\tau)\rho_{bn})U_n^{g\dagger}(t-\tau)\},\end{aligned} \tag{10}$$

$$\begin{aligned}\mathcal{E}_{n,j_n''j_n'''}(t,\tau;\rho_n) = \mathrm{Tr}_{bn}\{&U_n^g(t-\tau)\\ &\times(\rho_n(\tau)U_n(\tau)|j_n'''\rangle\langle j_n''|U_n^\dagger(\tau))U_n^\dagger(t-\tau)\}.\end{aligned} \tag{11}$$

Then, it is possible to show (see the Supplemental Material [23]) that Eq. (7) is equivalent to the following time evolution equation:

$$\begin{aligned}\frac{\partial}{\partial t}\langle j_n''|\sigma_{n,I}(t)|j_n'''\rangle = -\frac{1}{\hbar^2}\sum_{m\neq n}\sum_{j_n,k_m}\sum_{j_n',k_m'}J_{j_nk_m}J_{j_n'k_m'}\int_0^t d\tau\{&\langle k_m|\mathcal{I}_m(t,\tau)|k_m'\rangle\langle j_n'|\mathcal{E}_{n,j_n''j_n'''}(t,\tau;\rho_n)|j_n\rangle\\ &+\langle k_m'|\mathcal{I}_m^\dagger(t,\tau)|k_m\rangle\langle j_n|\mathcal{E}_{n,j_n'''j_n''}^\dagger(t,\tau;\rho_n)|j_n'\rangle-\langle j_n'|\mathcal{I}_{n,j_n'''j_n''}^\dagger(t,\tau)|j_n\rangle\langle k_m|\mathcal{E}_m^\dagger(t,\tau;\rho_m)|k_m'\rangle\\ &-\langle j_n|\mathcal{I}_{n,j_n''j_n'''}(t,\tau)|j_n'\rangle\langle k_m'|\mathcal{E}_m(t,\tau;\rho_m)|k_m\rangle\}.\end{aligned} \tag{12}$$

The GME for the MED, $p_n(t) = \sum_{j_n}\langle j_n|\sigma_{n,I}(t)|j_n\rangle$, can be obtained by summing the diagonal components of Eq. (12) and utilizing the fact that $\mathcal{I}_n(t,\tau) = \sum_{j_n''}\mathcal{I}_{n,j_n''j_n''}(t,\tau)$ and $\mathcal{E}_n(t,\tau;\rho_n) = \sum_{j_n''}\mathcal{E}_{n,j_n''j_n''}(t,\tau;\rho_n)$, yielding

$$\begin{aligned}\frac{\partial}{\partial t}p_n(t) = -\frac{1}{\hbar^2}&\sum_{m\neq n}\sum_{j_n,k_m}\sum_{j_n',k_m'}J_{j_nk_m}J_{j_n'k_m'}\\ &\times 2\mathrm{Re}\int_0^t d\tau\{\langle k_m|\mathcal{I}_m(t,\tau)|k_m'\rangle\langle j_n'|\mathcal{E}_n(t,\tau;\rho_n)|j_n\rangle\\ &-\langle j_n|\mathcal{I}_n(t,\tau)|j_n'\rangle\langle k_m'|\mathcal{E}_m(t,\tau;\rho_m)|k_m\rangle\}.\end{aligned} \tag{13}$$

Higher order versions of this equation can be obtained from Eq. (5) by following similar procedures including higher than second-order terms [25,32,33]. In the limit where each module consists of a single chromophore, the GME-MED reduces to the GME for localized excitons [34,35].

Equation (13) is the main formal result of the present Letter, but its solution requires full knowledge of the total density operator of each module, due to the dependence of $\mathcal{E}_n(t,\tau;\rho_n)$ on $\rho_n(\tau)$. We now describe a generic approximation removing such dependence, which is implicit in applications employing MC-FRET rates in the PME [14,18,20] and is believed to be appropriate for many natural photosynthetic systems. To simplify the argument, we shall assume that all H_n are time independent. Then, $U_n(t,\tau) = U_n(t-\tau)$ and $\mathcal{I}_n(t,\tau) = \mathcal{I}_n(t-\tau,0) \equiv \mathcal{I}_n(t-\tau)$. If the dynamics driving intramodule detailed balance are fast compared to the intermodule population dynamics, one may invoke the following steady state approximation: $\rho_n(\tau) \approx \rho_n^s p_n(\tau)$, where $\rho_n^s = e^{-\beta H_n}/\mathrm{Tr}_n\{e^{-\beta H_n}\}$. This does not imply *complete* time scale separation between intramodule and intermodule dynamics, and takes the full effect of exciton-bath entanglement into consideration through ρ_n^s. With this approximation, $\mathcal{E}_n(t,\tau) \approx \mathcal{E}_n^s(t-\tau)p_n(\tau)$, where $\mathcal{E}_n^s(t) = \mathrm{Tr}_{bn}\{U_n^g(t)\rho_n^s U_n^\dagger(t)\}$. Equation (13) then reduces to the following closed-form expression:

$$\begin{aligned}\frac{\partial}{\partial t}p_n(t) = \sum_{m\neq n}\int_0^t d\tau\{&\mathcal{K}_{n\to m}(t-\tau)p_m(\tau)\\ &-\mathcal{K}_{m\to n}(t-\tau)p_n(\tau)\},\end{aligned} \tag{14}$$

where

$$\mathcal{K}_{n\to m}(t) = \frac{2}{\hbar^2}\mathrm{Re}\sum_{j_n,k_m}\sum_{j'_n,k'_m} J_{j_n k_m} J_{j'_n k'_m} \times \langle k_m|\mathcal{I}_m(t)|k'_m\rangle\langle j'_n|\mathcal{E}^s_n(t)|j_n\rangle. \quad (15)$$

The GME-MED of Eq. (14) can now be solved employing the predetermined kernels of Eq. (15). Alternatively, a time-local version of Eq. (14) can also be derived following a similar step but utilizing the cumulant expansion approach [36]. This results in

$$\frac{\partial}{\partial t}p_n(t) = \sum_{m\neq n}\{W_{m\to n}(t)p_m(t) - W_{n\to m}(t)p_n(t)\}, \quad (16)$$

where $W_{n\to m}(t) = \int_0^t d\tau \mathcal{K}_{n\to m}(\tau)$. In the Markovian limit where all the intramodule exciton dynamics are much faster than the intermodule dynamics, both Eqs. (14) and (16) become equivalent and reduce to the PME with the following MC-FRET rate [22]:

$$W_{n\to m}(\infty) = \sum_{j_n k_m}\sum_{j'_n k'_m} J_{j_n k_m} J_{j'_n k'_m} \int d\omega E^{j'_n j_n}_n(\omega) I^{k_m k'_m}_m(\omega), \quad (17)$$

where $I^{k_m k'_m}_m(\omega) = \int_{-\infty}^{\infty} dt e^{i\omega t}\langle k_m|\mathcal{I}_m(t)|k'_m\rangle$ and $E^{j'_n j_n}_n(\omega) = 2\,\mathrm{Re}\int_0^{\infty} dt e^{-i\omega t}\langle j'_n|\mathcal{E}^s_n(t)|j_n\rangle$. This analysis clarifies the assumptions involved in the use of MC-FRET in PME (see also Ref. [37]), while also providing a non-Markovian generalization of that approach.

As a simple demonstration of accuracy, we consider a system consisting of bacteriochlorophylls (BChls) 1–4 in the Fenna-Matthews-Olson (FMO) complex and its protein bath, using parameters adopted from previous works [6,8] and modeling them as a two-module system [Fig. 2(a)]. The exciton Hamiltonian of each module is given by $H^e_n = E_{1_n}|1_n\rangle\langle 1_n| + E_{2_n}|2_n\rangle\langle 2_n| + \Delta_n(|1_n\rangle\langle 2_n| + |2_n\rangle\langle 1_n|)$, for $n = 1, 2$. Any type of spectral density for the bath can be used for the GME-MED. However, in order to make a comparison with the hierarchical equation of motion (HEOM) approach [38], which is limited to the Ohmic-Drude spectral density [6,8], we use the same spectral density, assuming the usual site-local reorganization energy of $\lambda = 35\ \mathrm{cm}^{-1}$ and Drude cut off at $\hbar\omega_c = 106\ \mathrm{cm}^{-1}$. The resulting modular excitonic densities calculated for two different initial conditions, one starting from $|1_1\rangle$ and the other starting from $|2_1\rangle$ are shown in Fig. 2 as blue and red dashed lines, respectively, at $T = 150$ and 300 K. Although the exciton population at each BChl is sensitive to the initial condition and exhibits strongly coherent behavior (see insets), the dynamics of modular exciton density is monotonic and much less sensitive to the initial condition.

Employing Eq. (16), the time-dependent MED was then calculated with two approximations for Eq. (15). The first

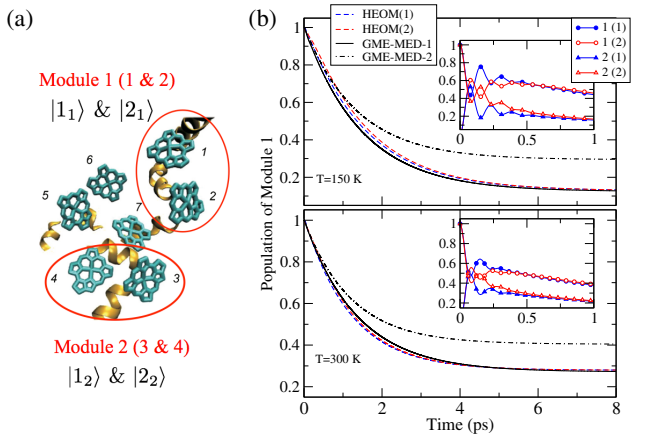

FIG. 2 (color online). (a) Decomposition of the first four BChls of FMO complex into two modules. The parameters defining H^e_n and H_c (all in cm^{-1}) are $E_{1_1} = 12\,400$; $E_{2_1} = 12\,520$; $E_{1_2} = 12\,200$; $E_{2_2} = 12\,310$; $\Delta_1 = -87$; $\Delta_2 = -53$; $J_{1_1 1_2} = 5$; $J_{1_1 2_2} = -5$; $J_{2_1 1_2} = 30$; $J_{2_1 2_2} = 8$. (b) Time-dependent populations of module 1 calculated with HEOM and with two different approximations for GME-MED. Insets show HEOM populations at each BChl. In all figures, numbers within parentheses represent the site of initial excitation.

neglects the off-diagonal elements of exciton-bath couplings in the exciton basis, while including all the diagonal exciton-vibrational terms (GME-MED-1). The second employs a second-order time-local quantum master equation approach neglecting initial exciton-bath coupling (GME-MED-2). Detailed expressions are provided in the Supplemental Material [23]. The results in Fig. 2(b) show excellent agreement of GME-MED-1 with the corresponding HEOM populations, both in the initial times and the steady state limits. In contrast, the GME-MED-2 results are much less accurate.

The excellent agreement of GME-MED-1 with HEOM at both low and room temperatures suggests that nonequilibrium effects, intermodule nonadiabatic couplings, and intermodule quantum coherence, none of which are fully accounted for here, have minor effects. Furthermore, comparison with the results in the Markovian limit (not shown) confirms that non-Markovian effects are also not significant. On the other hand, the relatively poor performance of GME-MED-2 demonstrates the importance of an accurate description of the exciton-bath coupling, some of which can be improved through nonperturbative treatment of the initial condition through analytic continuation from imaginary time [37]. These results illustrate the importance of using sufficiently accurate line shape expressions for PME calculations [14,17–20] to attain reliable accuracy.

As a further example demonstrating the capability of GME-MED in simulating large scale systems comparable to those studied recently by phenomenological approaches [20,39,40], we have calculated the exciton population dynamics between a pair of B850 rings in adjacent LH2

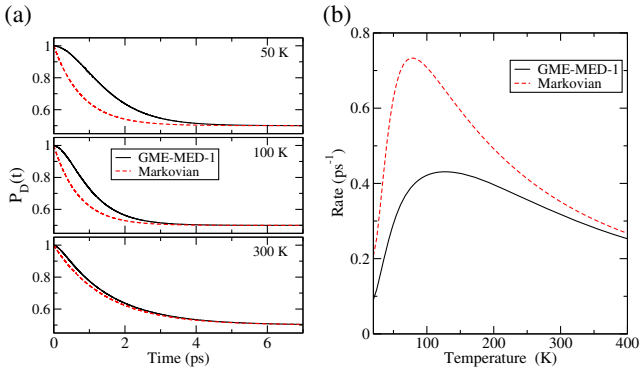

FIG. 3 (color online). Exciton dynamics between donor (D) and acceptor (A) B850 units separated by the center-to-center distance of 80 Å. (a) Time-dependent exciton population at the donor B850 unit. (b) Plot of effective forward rate k_{eff} (see text and [23]) from donor to acceptor with temperature. The black solid line is based on GME-MED-1 and the red dashed line its Markovian limit rate, which corresponds to the PME with MC-FRET rates.

light harvesting complexes of a purple bacterium, *Rps. Acidophila*. Each ring constitutes a module containing 18 bacteriochlorophyll molecules, for a total of 36 chromophores. Each B850 ring is described by a well-tested exciton Hamiltonian and spectral density [3]. The inter-B850 BChl electronic couplings are given by transition dipole interactions, which is an accurate description at the typical distances in *Rps. Acidophila* (≥ 2.5 nm). Figure 3(a) shows the time dependence of exciton population in the donor B850 ring at three different temperatures calculated by GME-MED-1 (black solid lines) and by its Markovian limit, PME with MC-FRET rates (red dotted lines). At short times we see significant differences between the GME-MED and MC-FRET curves, which reflect the influence of the non-Markovian bath dynamics in the GME-MED description compared to the Markovian dynamics assumed in MC-FRET theory. Figure 3(b) shows the temperature dependence of the effective forward rate for GME-MED-1, $k_{\text{eff}} = P_A(\infty)/\tau_{tr}$, where τ_{tr} satisfies the condition of $\ln[P_D(\tau_{tr}) - P_A(\tau_{tr})P_D(\infty)/P_A(\infty)] = -1$ (see the Supplemental Material [23]), and the Markovian MC-FRET rate, $W_{D\to A}(\infty)$. We note that the effective rate reflecting the non-Markovian dynamics is significantly smaller than the Markovian rate at low temperatures, but approaches it at room temperatures and above. GME-MED-1 is much more efficient than the HEOM approach [10] (each calculation takes only a few seconds on a typical desktop computer), and makes it possible to simulate excitonic energy transfer between e.g., larger aggregates of LH2 with incorporation of energetic disorder, a key feature necessary to explain experimental results [41,42] and to understand the robustness of energy transfer dynamics in light harvesting systems over a broad range of temperature.

In summary, we have presented a general derivation of a generalized master equation describing the quantum evolution of exciton density in modular materials, GME-MED, which provides a rigorous derivation of the PME with MC-FRET rates and also offers its non-Markovian generalization. As a proof of principle demonstration, we showed that this approach gives an accurate description of population dynamics between modules in subcomplexes of FMO within which significant electronic coherence exists. As a further demonstration of its applicability to large scale systems, we provided results for exciton energy transfer between B850 units of LH2 complexes in purple bacteria that revealed the significance of non-Markovian effects over a range of temperatures. Taken together, these demonstrations support the GME-MED approach as a novel route to calculation of long-range transfer of excitonic energy between modules within which electronic coherence is present.

This work was supported by Defense Advanced Research Projects Agency under Award No. N66001-09-1-2026. S. J. also acknowledges support by the National Science Foundation CAREER award (Grant No. CHE-0846899), the Office of Basic Energy Sciences, Department of Energy (Grant No. DE-SC0001393), and the Camille Dreyfus Teacher Scholar Award. S. H. also acknowledges support by a DOE Office of Science Graduate Fellowship. G. R. F. also acknowledges support from the Director, Office of Science, Office of Basic Energy Sciences, of the U.S. Department of Energy under Contract No. DE-AC02-05CH11231. We thank H. Choe for rendering the image of Fig. 1.

*Corresponding author.
Seogjoo.Jang@qc.cuny.edu

[1] X. Hu, T. Ritz, A. Damjanovic, F. Autenrieth, and K. Schulten, Q. Rev. Biophys. **35**, 1 (2002).
[2] R. E. Blankenship, *Molecular Mechanism of Photosynthesis* (Blackwell Science, Oxford, England, 2002).
[3] S. Jang, M. D. Newton, and R. J. Silbey, J. Phys. Chem. B **111**, 6807 (2007).
[4] P. Rebentrost, M. Mohseni, I. Kassal, S. Lloyd, and A. Aspuru-Guzik, New J. Phys. **11**, 033003 (2009).
[5] F. Caruso, A. W. Chin, A. Datta, S. F. Huelga, and M. B. Plenio, Phys. Rev. A **81**, 062346 (2010).
[6] S. Hoyer, A. Ishizaki, and K. B. Whaley, Phys. Rev. E **86**, 041911 (2012).
[7] J. L. Wu, F. Liu, Y. Shen, J. S. Cao, and R. J. Silbey, New J. Phys. **12**, 105012 (2010).
[8] A. Ishizaki and G. R. Fleming, Proc. Natl. Acad. Sci. U.S.A. **106**, 17255 (2009).
[9] P. Huo and D. F. Coker, J. Phys. Chem. Lett. **2**, 825 (2011).
[10] J. Strümpfer and K. Schulten, J. Chem. Phys. **134**, 095102 (2011).
[11] J. Strümpfer and K. Schulten, J. Chem. Phys. **137**, 065101 (2012).

[12] B. Hein, C. Kreisbeck, T. Kramer, and M. Rodriguez, New J. Phys. **14**, 023018 (2012).
[13] C. Kreisbeck and T. Kramer, J. Phys. Chem. Lett. **3**, 2828 (2012).
[14] T. Ritz, S. Park, and K. Schulten, J. Phys. Chem. B **105**, 8259 (2001).
[15] M. K. Sener, S. Park, D. Lu, A. Damjanović, T. Ritz, P. Fromme, and K. Schulten, J. Chem. Phys. **120**, 11183 (2004).
[16] M. Yang, A. Damjanović, H. M. Vaswani, and G. R. Fleming, Biophys. J. **85**, 140 (2003).
[17] V. I. Novoderezhkin, A. Marin, and R. van Grondelle, Phys. Chem. Chem. Phys. **13**, 17093 (2011).
[18] T. Renger, Photosynth. Res. **102**, 471 (2009).
[19] T. Renger, M. E. Madjet, A. Knorr, and F. Müh, J. Plant Physiol. **168**, 1497 (2011).
[20] D. I. G. Bennett, K. Amarnath, and G. R. Fleming, J. Am. Chem. Soc. **135**, 9164 (2013).
[21] G. D. Scholes, X. J. Jordanides, and G. R. Fleming, J. Phys. Chem. B **105**, 1640 (2001).
[22] S. Jang, M. D. Newton, and R. J. Silbey, Phys. Rev. Lett. **92**, 218301 (2004).
[23] See Supplemental Material at http://link.aps.org/supplemental/10.1103/PhysRevLett.113.188102, which includes Refs. [24–28], for details of the derivations of Eqs. (5) and (12) and of the implementations of GME-MED-1 and GME-MED-2.
[24] N. G. van Kampen and I. Oppenheim, J. Stat. Phys. **87**, 1325 (1997).
[25] S. Jang, J. Cao, and R. J. Silbey, J. Chem. Phys. **116**, 2705 (2002).
[26] S. Jang, J. Cao, and R. J. Silbey, J. Phys. Chem. B **106**, 8313 (2002).
[27] S. Jang and R. J. Silbey, J. Chem. Phys. **118**, 9312 (2003).
[28] P. Kumar and S. Jang, J. Chem. Phys. **138**, 135101 (2013).
[29] W. H. Miller, J. Phys. Chem. A **105**, 2942 (2001).
[30] N. Makri, Annu. Rev. Phys. Chem. **50**, 167 (1999).
[31] S. Ganapathy, G. T. Oostergetel, P. K. Wawrzyniak, M. Reus, A. Gomez Maqueo Chew, F. Buda, E. J. Boekema, D. A. Bryant, A. R. Holzwarth, and H. J. M. de Groot, Proc. Natl. Acad. Sci. U.S.A. **106**, 8525 (2009).
[32] A. A. Golosov and D. R. Reichman, Chem. Phys. **296**, 129 (2004).
[33] V. May, J. Chem. Phys. **129**, 114109 (2008).
[34] V. M. Kenkre and R. S. Knox, Phys. Rev. B **9**, 5279 (1974).
[35] T. Renger, V. May, and O. Kühn, Phys. Rep. **343**, 137 (2001).
[36] F. Shibata and T. Arimitsu, J. Phys. Soc. Jpn. **49**, 891 (1980).
[37] L. Banchi, G. Costagliola, A. Ishizaki, and P. Giorda, J. Chem. Phys. **138**, 184107 (2013).
[38] A. Ishizaki and G. R. Fleming, J. Chem. Phys. **130**, 234111 (2009).
[39] T. Fujita, J. C. Brookes, S. K. Saikin, and A. Aspuru-Guzik, J. Phys. Chem. Lett. **3**, 2357 (2012).
[40] J. Huh, S. K. Saikin, J. C. Brookes, S. Valleau, T. Fujita, and A. Aspuru-Guzik, J. Am. Chem. Soc. **136**, 2048 (2014).
[41] V. Sundstrom, T. Pullerits, and R. vanGrondelle, J. Phys. Chem. B **103**, 2327 (1999).
[42] R. Agarwal, A. H. Rizvi, B. S. Prall, J. D. Olsen, C. N. Hunter, and G. R. Fleming, J. Phys. Chem. A **106**, 7573 (2002).